GeoLab, a Measurement System for the Geotechnical Characterization of Polluted Submarine Sediments

(Article begins on next page)

20 April 2024

GeoLab, a Measurement System for the Geotechnical Characterization of Polluted Submarine Sediments

Francesco Adamo[1], Gregorio Andria[1], Osvaldo Bottiglieri[2], Federica Cotecchia[2], Attilio Di Nisio[1],

Daniela Miccoli[2], Francesca Sollecito[2], Maurizio Spadavecchia[1], Francesco Todaro[2], Amerigo

Trotta[1], Claudia Vitone[2]

[1] *Polytechnic University of Bari - Department of Electrical and Computer Science Engineering,*
Bari, Italy, gregorio.andria@poliba.it

[2] *Polytechnic University of Bari - Department of Civil, Environmental, Land, Building Engineering*
and Chemistry, Bari, Italy, federica.cotecchia@poliba.it

Abstract **– In this paper an integrated system (hardware and software), named GeoLab, for geotechnical measurement on submarine contaminated sediments is described; GeoLab permits to reduce the probability of human mistakes often made during long and repetitive manual operations and, to increase speed, accuracy, and productivity in geotechnical laboratory tests. A new, suitable management software was developed to permit the communication with different data acquisition platforms and to easily adapt software in case of changes in the laboratory procedures.**

Keywords: Geotechnical Measurements, Automated Test System, Marine Sediments Characterization

I.   INTRODUCTION

In the last decades, growing attention has been paid to monitor the sea water quality and coasts status; several studies have been carried out to propose new methods and systems for the accurate measurement of environmental parameters to obtain models of the sediments permitting to analyse dynamic phenomena closely linked to marine pollution [1]-[7]. At the same time, the need of a rational approach to environmental monitoring requiring the aggregation of data in distributed database able to store all information about each matrix of interest has become mandatory. All the data must be traceable and should permit an efficient processing of such massive database.

The reference domain for this work falls into the geotechnical characterization of the submarine sediments from a heavily polluted basin; the final goal is to define the best strategy for their recovery. In this context,

29 accurate measurements on submarine contaminated sediments are of great importance for selecting the most

30 sustainable strategies for both the remediation and management of environmental contamination, aimed to

31 both reduce health risks and to preserve the ecosystem. This work focuses on the geotechnical laboratory tests

32 that permit to investigate the main soil mechanical properties, such as compressibility and shear strength. In

33 particular, the one-dimensional consolidation and compressibility properties of the soils are commonly derived

34 by means of odometer test (OT), whereas their shear strength parameters can be determined either through

35 direct shear tests (DS) or by using triaxial tests (TTs) [8].

36 This paper deals with the development of a measurement system installed into a suitable geo-mechanical

37 laboratory, that has been validated for the characterisation of the polluted submarine sediments taken from the

38 Mar Piccolo in Taranto (South of Italy, Fig. 1), that is part of an area declared as *"at high risk of environmental*

39 *crisis"* by the Italian government. Due to the long-lasting industrial activities, this marine basin results to be

40 highly contaminated, by both heavy metals and organic pollutants [9], [10]. This finding prompted a

41 multidisciplinary investigation of the in-situ chemical, hydrological, hydrogeological and geological

42 conditions of the basin and the assessment of the geotechnical and chemo-mechanical properties of the

43 sediments by laboratory testing.

44 The proposed measurement system was employed in an extensive geotechnical investigation campaign, on

45 undisturbed samples of sediments taken up to about 30 m below the seafloor, along nineteen vertical profiles

46 drilled in the Mar Piccolo ([4], [11]-[13], Fig. 1). The specific characteristics of such sediments have required

47 the development of innovative solutions for laboratory testing, so that some novelties have been introduced in

48 the phase of soil sampling and in testing equipment, to preserve both the human safety and the sample quality

49 (Fig. 2 and 3, [14]). The assessment of both the compression and shearing behaviour of the shallowest and

50 ultra-soft strata of sediments has been carried out by means of standard equipment and procedures that,

51 sometimes, have been modified to both efficiently manage constrains given by potential contamination and

52 the presence of marine water. Moreover, an original acquisition system has been designed. Such system is

53 composed by a purposely developed hardware and a related suite of software programs, able to both acquire

54 and process data coming from transducers used for different tests. The new acquisition system allowed to

55 increase speed and accuracy, reduces the risk of human mistakes and, more in general, improves the

56 productivity of the geotechnical investigation.

Fig.   1 - Gulf of Taranto and area of Mar Piccolo in the South of Italy
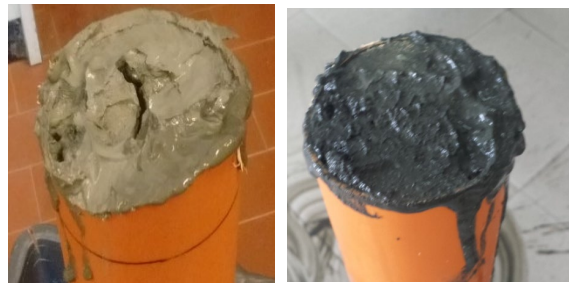
Fig.   2   - Soft marine sediments from the Mar Piccolo of Taranto.

Fig.   3 – Operator involved in the extrusion of the contaminated sediments from the samplers.

Since about twenty years different solutions had studied by scientific and technical community, in order to have automated and reliable systems for soil mechanics testing [17]-[23]. In most frameworks the management software is usually supplied by the manufacturer bundled with hardware, thus the customer is constrained to use a complete but "closed" testing equipment [22]. This approach evidently implies a strong dependency on

62   the specific vendor for any upgrade of products and services and unable one to use other products (or software)

63   without switching costs. The major strength of the realized framework, instead, is the high degree of

64   reconfigurability, so the researchers will be able to develop and test new procedures or innovative algorithms

65   to extract information from acquired data and finally to share results on different platforms [15], [24]. Other

66   elements of novelties, as widely described in Section III, are respectively: the design of a low noise/high

67   stability power supply for transducers' excitation and the develop of a highly reliable management software

68   based on data buffering to allow a different rate of data consumption for different test or different channels

69   among the same trial.

II.   TEST PROCEDURES

71   The OT reproduces, in the laboratory, the one-dimensional compression of soil due to axial loading. It is

72   performed to investigate soil compression and swelling (i.e. the relation between effective stress and

73   volumetric strain) or consolidation (i.e. the relation between compression and effective stress), on an

74   undisturbed cylindrical soil specimen placed when it is restrained laterally while subjected to the application

75   of axial loading steps. Under these conditions, the soil straining and the water flow are allowed only in the

76   vertical direction. Two classes of test can be distinguished: stress-controlled loading and strain-controlled

77   loading [25], [26]. The test procedure has been standardized in BS 1377-5 [28], and ASTM D2435 [29]. A

78   sketch of the OT apparatus is reported in Fig. 4a.

79   In the basic version of the OT apparatus, the oedometer cell (Fig. 4b) is placed on a rigid aluminium base and a

80   loading yoke allows the load transmission from a lever arm carrying the weights to the specimen top cap. The

81   oedometer cell consists of a rigid stainless-steel ring containing the specimen, which is in contact with two

82   porous stones at the top and the bottom to allow double drainage of the pore fluid. Two discs of filter paper

83   are also placed between the specimen and the two porous stones to prevent their clogging. The soil specimen

84   size (50 mm diameter, 20 mm high) used for the work had diameter-height ratio greater than two, in order to

85   reduce the effects of side friction [30].

86   During each loading step, the vertical compression or swelling of the specimen under the actual stress is

87   measured by means of a Linear Displacement Transducer (LDT), operating on the loading cap and firmly

88   mounted at the top of the machine (Fig. 4c). When the axial stress is applied, the sample of initial height H_0

89   deforms vertically with time. It ultimately settles of an amount ΔH when the excess pore-water pressure is

90   "completely" dissipated, according to the so-called consolidation process. As lateral strain is restricted by the

91   stiff ring ($\varepsilon_r = \varepsilon_y = 0$), the volumetric strain, ε_{vol}, coincides with the axial strain, ε_z and it is computed

92   according to equation (1):

$$\varepsilon_{vol} = \varepsilon_x + \varepsilon_y + \varepsilon_z = \varepsilon_z = -\frac{\Delta H}{H_0} \qquad (1)$$

93 The soil compression indexes during the loading and unloading phases (i.e. C_c and C_s respectively), are

94 usually expressed as the ratio between the total variation of void ratio, Δe, and the corresponding loading

95 effective stress increment in the semi-logarithmic plane (i.e. $\Delta \log \sigma' v$):

$$Cc, Cs = -\frac{\Delta e}{\Delta log \sigma' v} \qquad (2)$$

96 where the void ratio, e, is the ratio between the volume of voids and the volume of the soil particles. Δe is

97 derived from the volumetric strain and the measured initial void ratio of the specimen, e_0:

$$\varepsilon_{vol} = -\frac{\Delta e}{1 + e_0} = -\frac{e_- e_0}{1 + e_0} \qquad (3)$$
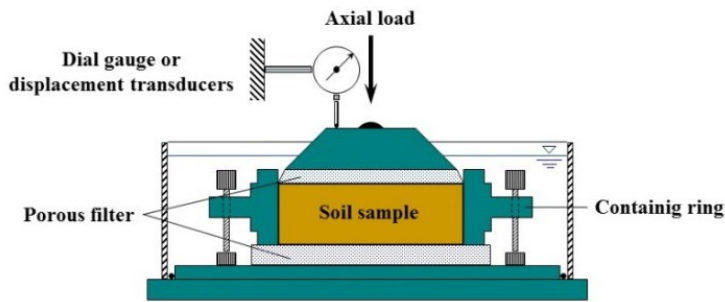
a)

b)   c)

Fig.   4 - Sketch of an Oedometer Test apparatus (OT) (a); photographs of the oedometer cell components
(b) and of one of the apparatuses located in the geotechnical laboratories of the Polytechnic University of
Bari(c).

98 As for the soil compressibility, also the shear strength parameters can be determined by means of laboratory

99 tests on undisturbed specimens taken from representative samples of the in-situ soil. One of these tests, is the

100   Direct Shear Test (DST), whose apparatus is shown in Fig. 5. According to the test procedures, that are detailed

101   in BS 1377-7, 1377-8 [28] and in ASTM D3080 [31], the specimen is placed in a metal box (shear box),

102   between two porous plates to allow free drainage. The shear force T exhibited by the soil is then measured

103   by means of a load cell, while the corresponding shear displacement and the change in the specimen height are

104   measured by means of two LDTs, installed on the box and on the loading cap, respectively [25]-[27]. It is

105   worth noting that during the initial phase of the work, the reliability of the developed system has been verified

106   by installing on each device used (OT, DS) both electrical and mechanical transducers and comparing the

107   corresponding measurements (as better described in Section IV).

108   Both the values of the shear stress, τ, obtained as force, T, divided by the cross-section area A, and the

109   vertical displacements, ΔH, recorded during the shear phase, are plotted against the horizontal displacements,

110   ΔS. The values of the maximum shear stress recorded for each specimen are plotted against the normal effective

111   stress. The effective shear strength parameters are then obtained from the fitting of the critical state points.
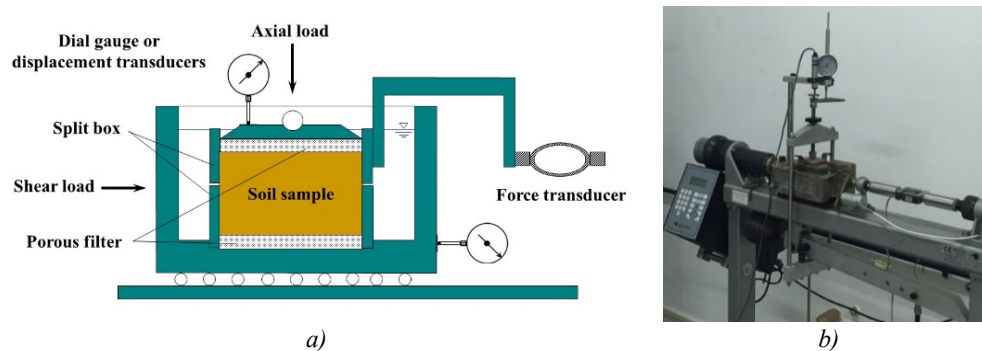
112

Fig.   5 - Direct shear test apparatus: sketch (a) and photograph (b) of one of the apparatuses present in the geotechnical laboratories of the Polytechnic University of Bari.

113   The most widely used test to determine the soil shear strength parameters is the TT test. It is versatile because,

114   by changing some test conditions, a wide variety of stress paths may be performed [30]. The main features of

115   the triaxial apparatus are shown in Fig. 7, and the TT procedure is reported in both ASTM [32] and BS codes

116   of practice [28]. Cylindrical specimens 38 mm diameter – 76 mm high have been enclosed in a latex membrane,

117   placed on a base platen and sealed at the top and bottom by o-rings. The specimens are placed in a cylindrical

118   cell full of water under confining pressure, σ_r, in the cell there is also a submergible load cell, to measure the

119   axial force, F_a, applied to the specimen in addition to the cell pressure. With respect to the DS test, the TT

120   apparatus allows to control the drainage conditions to measure of the pore water pressure. The simplest TT

121   consists of two phases: isotropic compression and shearing. During the first one, the specimen is subjected to

122   an all-round fluid pressure in the cell and consolidation can take place in a drained test as the pore water can

123   freely drain from the specimen to a volume gauge. The second phase is performed until either the specimen

124   assumes a typical bottle-shape or one or more sliding planes are visible on the specimen surface([25]-[27],

125   [33], Fig. 7). This can be obtained by moving the sample pedestal upwards at a constant rate and pushing the

126   top of the specimen against the stationary submergible load cell. Five transducers are required to perform

127   standard TT tests: two pressure transducers for cell and pore water pressure respectively, a submergible load

128   cell, a volume gauge fitted with a LVDT to measure the volume variation of the specimen, and another LVDT

129   to measure the axial deformation of the specimen during the shearing phase.

130   The isotropic compressibility, derived by TT, is usually simply related to the one-dimensional compression

131   derived by OT [33]. The shear strength parameters of the TT and DST could be comparable, even if the

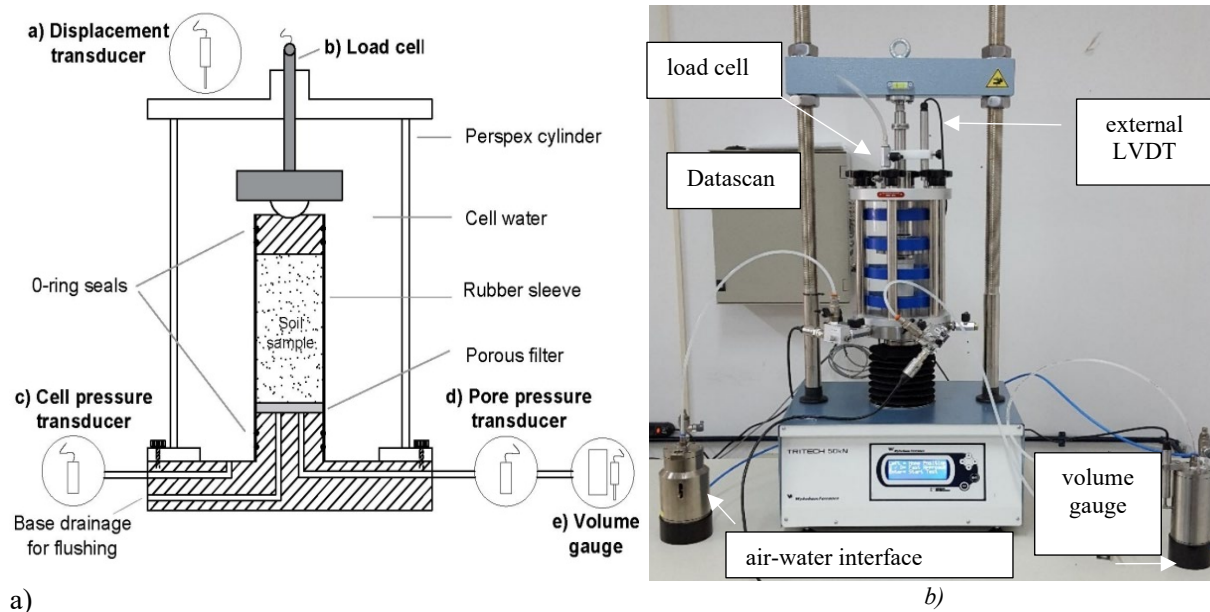132   different test conditions lead to different results.

133

Fig.   6 - Triaxial apparatus: sketch (a) and photograph (b) of one of the apparatuses present in the geotechnical laboratories of the Polytechnic University of Bari.

Fig.   7 - Photographs of the specimens at the end of the triaxial tests.

III.   THE MEASUREMENT SYSTEM

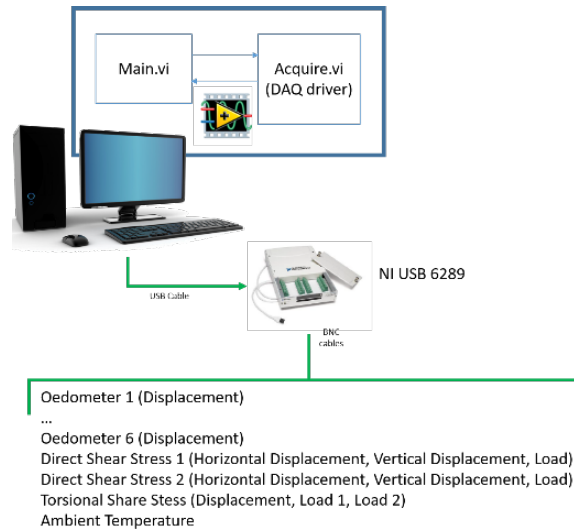The conceptual scheme of the whole measurement system is reported in Fig. 8.

Fig. 8 - Conceptual scheme of the proposed system

Test equipment includes several transducers: Linear Variable Differential Transformers (LVDTs) are used in triaxial apparatus to measure axial deformation; they have internal stabilization of the power supply and a 2.2 V output range. Linear Displacement Transducers (LTDs) based on strain-gauge bridge instead are used to measure specimen deformation in both oedometers (vertical displacement) and direct shear stress test apparatuses (vertical and horizontal displacement).

The strain-gauge bridge of these sensors is excited through a high stability 10 V power supply described in subsection 3.2 which has been purposely designed. S-shaped load cells found in DST apparatus, submergible load cells and pressure sensors, used in TT tests are also excited through the same high stability power supplies. To simplify laboratory management, all the sensors have been cabled with the same 5-pole connector and wall-mounted cabinets have been designed.

3.1   SOFTWARE SUITE

The control software of the new measurement system was developed in LabVIEW® (by National Instruments Corp.), to allow the easy interfacing with different data acquisition hardware platforms and to simplify both the software reconfiguration and the hardware replacement. Generally speaking, it represents a helpful tool to manage several testbeds based on local and remotely controlled instruments (USB, IEEE488, Ethernet, etc.) and data acquisition devices, ranging from remote sensing [34]-[36], energy monitoring [37], up to automotive

154 [38] or devices test and characterization [39], [40] only to make some examples.

155 The software suite manages all tests and the sensors calibration procedures, showing as much information as

156 possible and keeping track of all the history of the measurands. In detail, four software modules were created:

157 • OT and DST transducers calibration;

158 • TT transducers calibration;

159 • OT and DST Management Software

160 • TT Management Software

161 Each module has a user-friendly interface and was programmed to acquire signals from the transducers

162 mounted on each testing apparatus and to monitor the change of each measurand (i.e. displacement, load and

163 pressure) when the specimen is loaded. Moreover, some parameters such as temperature, sensor supply voltage

164 and offset of the acquisition channel can be acquired, using suitable accessories, to study their influence on

165 measurements.

166 Two different calibration software modules were developed because of different DAQ boards were used

167 respectively for one-dimensional (OT and DST) and TTs although the same workflow was used. When is run,

168 the calibration software acquires continuously voltage signal from the channel of the DAQ where the

169 transducer under calibration is connected. A graphical display shows the actual sampled buffer whereas two

170 numerical displays show the mean and the standard deviation of the signal. When these values are stable the

171 value of the measurands (read, for example, using a micrometre in the case of displacement transducer) is

172 manually input by the user thus the value of measurand and corresponding voltage are stored and directly

173 displayed. This procedure is generally repeated both for increasing and decreasing values, eventually many

174 times to assess hysteresis and repeatability errors. At the end of this process, slope, intercept and correlation

175 coefficient of the linear regression are automatically estimated. The software can estimate also nonlinear

176 models such as polynomial and exponential ones, or use different fitting methods, showing the fitting equation.
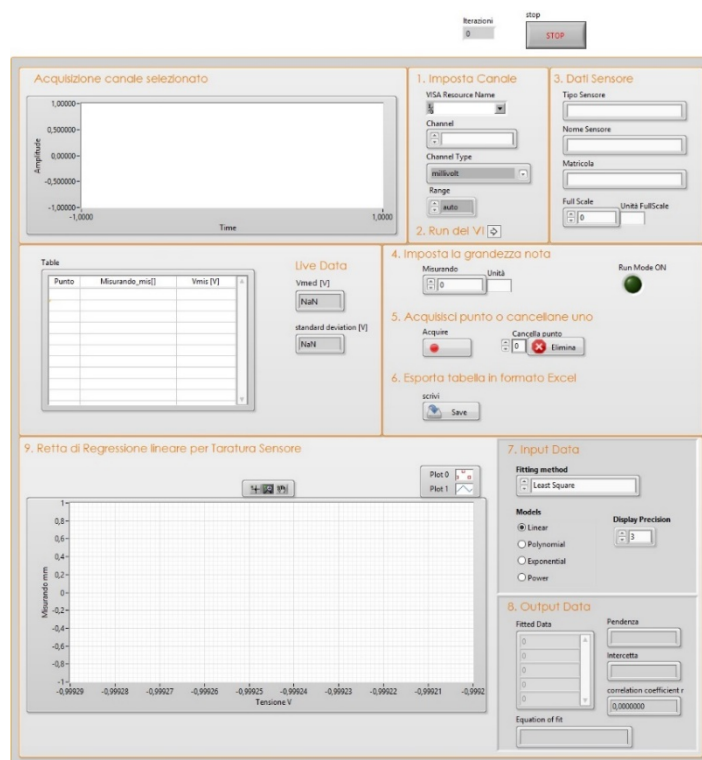
177

Fig.   9 - Screenshot of developed interface of calibration software for TT transducers

178 As reported in Fig. 9, the Management modules were subdivided in two subVIs, configuring a
179 producer/consumer situation from the data flow point of view. One is devoted to communicating with the DAQ
180 board thorough the proper driver and to acquire signals buffering them in a FIFO queue. Since geotechnical
181 experiments are generally long-lasting tests due to the very low soil permeability (i.e. the soil permeability, k,
182 varies between about 10^{-5} and 10^{-14} m/s), a fundamental sample rate of 0.1 s was considered sufficient to
183 analyse the fastest dynamic phenomena; thus, the sampling rate of each channel may be configured as a
184 multiple of this fundamental sampling time. Indeed, each measurement (each element of the queue) is the mean
185 over 1000 samples acquired at 10 kS/s sampling frequency to filter possible outliers and to improve the
186 measurement accuracy. Moreover, for DAQ board supporting this feature, the data acquisition is stopped every
187 30 minutes to perform an autocalibration to minimize errors due to thermal drift of the DAQ board.
188 The second one (i.e. the main VI) is responsible for the channels configurations and to route the data streamed
189 by the queue to the proper test. The OT-DST management software can simultaneously manage different tests:
190 six OTs, two DSTs, one torsion shear stress with a further channel used to monitoring the room temperature
191 for a total of sixteen differential channels. Whereas the TT Management Software can acquire transducers
192 from two different TTs or, better, simultaneously from: four pressure transducers, two submergible load cells,
193 two LVDTs, two volume gauges and some additional local transducers to acquire specific data such as the cell
194 temperature or local displacement directly on the soil specimen during the test. Anyway, each channel may be

195   set in term of channel type (Referenced Single Ended/Not Referenced Singe Ended/Differential), scale factor,

196   sample rate, etc. All test parameters are settable using a cluster containing basic information (calibration

197   constants, sampling rate, offset and mechanical zero, applied load, etc.). Some graphs reporting the transduced

198   variables for both the OT and DST measurement systems are shown in Figs. 10 and 11, respectively. The OT

199   interface shows the time variation of the vertical displacement, that is the evolution of the consolidation process

200   of the specimen during a single loading step. The DST interface shows the simultaneous evolution of both

201   vertical and horizontal displacements together with the shear strength recorded by the load cell.
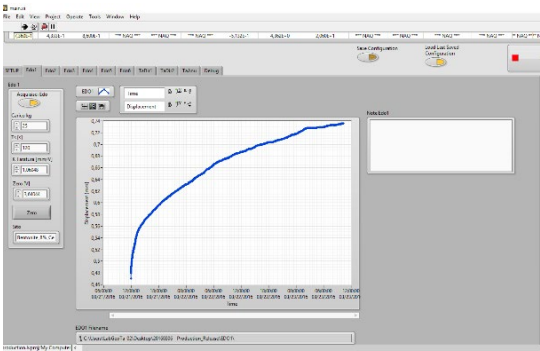
202

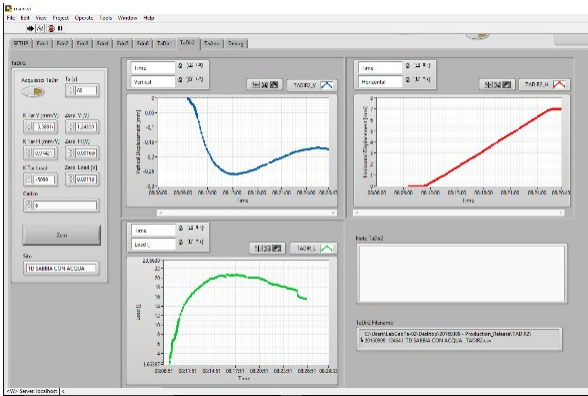*Fig.   10 - Screenshot of developed OT interface*

203

Fig. 11 - Screenshot of developed DST interface

204   In addition to the monitoring of variables with time (i.e. specimen volume, cell pressure, pore fluid pressure,

205   shear strength), a set of equations from soil mechanics has been implemented in the TT software to compute

206   the specimen properties from the input data. Some initial data, measured before the setting up of the specimen,

207   could be entered the box of the consolidation phase (Fig. 12a): the specimen geometry (i.e, diameter D_0; height,

208   H_0), the soil bulk unit weight, γ; the soil solids unit weight, γ_s, and the initial water content, w_0. The specimen

209   initial void ratio, e_0, which represents the volume of voids divided by the volume of soil particles, is computed

210   in the code by means of the following equation:

$$e_0 = \frac{\gamma_s (1 + w_0)}{\gamma} - 1 \qquad (4)$$

211

212   The box related to the sharing phase (Fig. 13b) requires the input data of the volumetric strain, $\varepsilon_{vol\,f}$, exhibited

213   by the specimen during the consolidation phase. The output data at the beginning of the shearing phase are the

214   current specimen size (i.e. diameter, D, height, H, volume, V, cross-section, A), the final void ratio, e_f, and the

215   final dry bulk unit weight, γ_d. The equations implemented in the code are:

$$V = V_0 - \varepsilon_{vol\,f} * V_0 \qquad (5)$$

$$D = \sqrt[3]{\frac{2 * V}{\pi}} \qquad (6)$$

$$A = \pi * \frac{D^2}{4} \qquad (7)$$

$$e_f = e_0 - \varepsilon_{vol} (1 + e_0) \qquad (8)$$

$$\gamma_d = \frac{\gamma_s}{1 + e_f} \qquad (9)$$
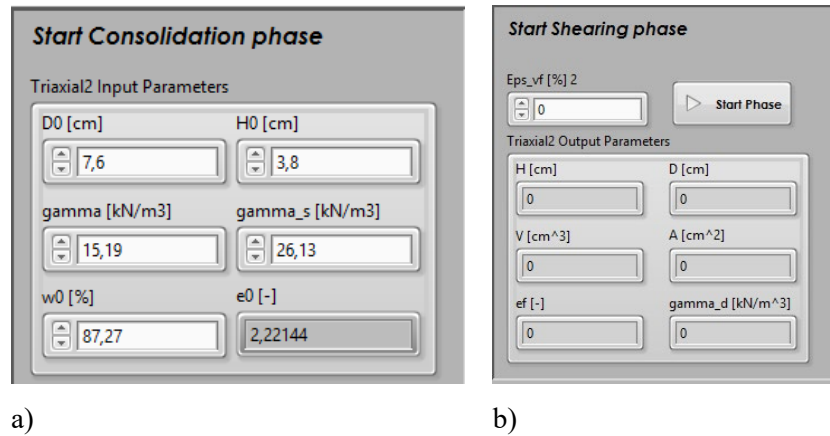
216

217

a)   b)

Fig.   12 – Screenshot of the developed TT interface for the computation of the specimen properties: a)
specimen properties computed at the beginning of the consolidation phase; b) specimen properties computed
at the beginning of the shearing phase.

218

219 All object values, proprieties and methods are exchanged between front panels and block diagrams using a set

220 of global variables and references to controls or indicators. This is the case, for example, to route data from

221 each transducer to the proper graph or log-file. This solution makes it possible to have a hardware-independent

222 software with a high degree of flexibility to front possible changes either in channel numbers or in the type of

223 trials.

224 Raw and scaled data are continuously stored in a Comma Separated Values (CSV) log file corresponding to a

225 single test apparatus with all calibration coefficients and timestamps, so that researchers can also post-process

226 data for further analysis [41], [42]. Each log file may receive data from one (in the case of OT) or more DAQ

227 channels depending on the test. Near real-time plots are available during the data acquisition.

228 One of the most interesting feature introduced with the system here presented is the remote monitoring through

229 networking techniques. The networking was mandatory also to allow the test control by different faraway

230 laboratories making possible the collaboration between interdisciplinary groups or the inter-laboratory data

231 validation. Then, different solutions have been developed ranging from the simple monitoring of the test by

232 means of a common web-browser to the full control of the testing interface using web-based or built-in
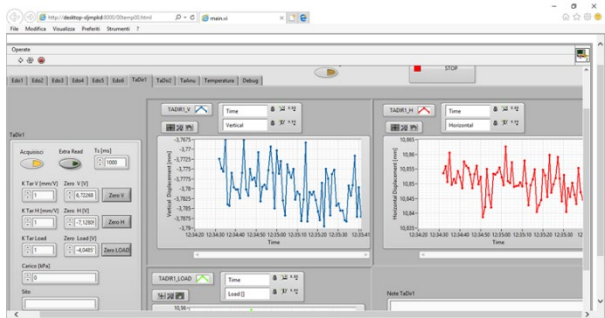
233 solutions.

234

Fig.   13 - Remote management of the OD test using an internet web browser

235 An optimal solution is the direct connection to the user interface of the management software by activating a

236 dedicated web server using features natively implemented in LabVIEW thus avoiding the use of third-party

237 software modules such internet browser, Remote Desktop or Virtual Network Computing. The main advantage

238 is the great responsivity of the user interface in terms of both response to remote commands and of low latency

239 in displaying of data graphs (Fig. 13).

240

241 3.2   HARDWARE PLATFORMS

242 From the hardware point of view, this research has required an intense work for the designing and prototyping

243 of the signal acquisition control boxes. One of the most difficult aspect of the work was related to the large

244 number of sensing points and to the long distances between the sensing points and the control PC; these aspects

245 had imposed the design of: wall-mounted boxes containing the DAQ devices and , a signal routing PCB

246 (printed circuit board) with per-channel configurable low-pass filters and precision high current voltage

247 references to excite the transducers.

248 Figures 14 to 17 show some pictures of the data-acquisition cabinets designed for this project. Each cabinet

249 contains a 13 V power supply, for powering LVDTs, and three voltage reference modules, for exciting

250 remaining transducers; 16 connection ports are available, where the voltage supplied to each port can be

251 selected among those available   (namely V1 = 13 V, V2' = V2''= 10 V, and V3 = 5 V) using a three-position

252 slider placed alongside each connection port (see Fig 14).

253

254

Fig. 14 - Side view of one of the new wall-mounted cabinets designed for this research

255

Fig. 15 - Internal view of one data acquisition cabinet based on a National Instruments' USB DAQ device

256   In particular, Fig. 15 shows a detail of the mains supply input connector and of the connectivity options to the
257   remote PC. In the different releases of control boxes built for this project only the USB and the serial
258   connectivity were used; the Ethernet connector was added as a spare option for future developments.
259   In Fig. 16 four panel-mounted digital voltmeters are visible; they were added to give the operator the
260   opportunity to see at a glance the internal main DC power supply output voltage as well as the output voltages
261   of up to three internal reference generators.

262

Fig. 16 - Detail of the main supply and connectivity options of the cabinet; digital voltmeters V1, V2', V2''
and V3 installed in order to monitor the various output voltages.

263
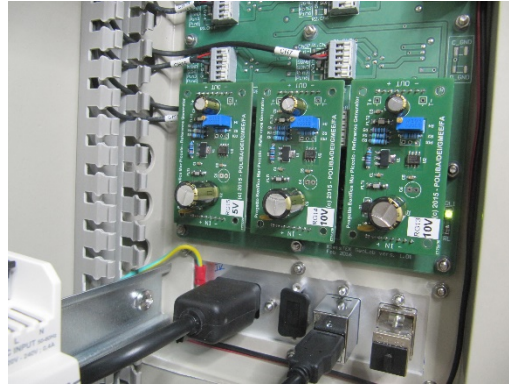
Fig. 17 - Detail of Fig. 16 showing the three precision voltage sources installed in the cabinet

264   The precision voltage reference source designed for this project is shown in Fig. 18; it consists of a Texas

265   Instruments' TL1431Q precision programmable reference [43], which drives a TLV1117 Low-Dropout

266   Voltage Regulator [44], used as an output power buffer; the output voltage is programmable by a fixed voltage

267   divider composed by two discrete 0.1% low TC (Thermal Coefficient) resistors, and finely tunable thanks to a

268   25 turns onboard trimmer. Also, to gain a better initial accuracy and temperature stability, room was left on

269   the PCB for a Vishay's 300144Z series Ultra High Precision Z-Foil Voltage Divider [45].

270   The output voltage must be adapted to the kind of sensors connected to the data acquisition box input channels,

271   thus on the routing PCB room for three different voltage reference modules was reserved and each input

272   channel can be switched at the output of one of these modules by means of an onboard slide switch. Also, the

273   voltage reference modules are modular since they have snap-in connectors for a quick and easy replacement

274   in case of failure or to modify the output voltage substituting the voltage divider resistors.

275
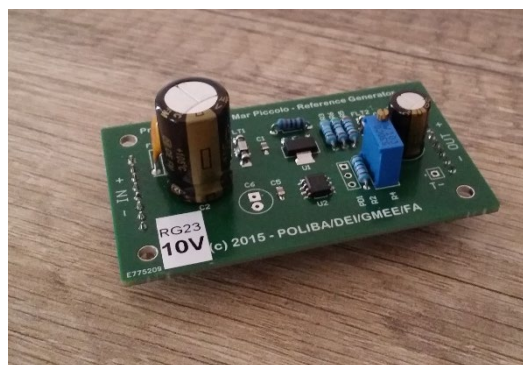
Fig.   18 – Image of one 10V voltage reference circuit

276   A laboratory characterization of these modules was performed using an automated test setup made by a

277   Hockerl & Hackl ZSHW20D programmable load, a Keysight E3631A triple output power supply used as a

278   primary power source and a Keysight E34401A benchtop $6^{1/2}$ digits digital multimeter used to accurately

279   measure the module output voltage under the different load conditions, with output current spanning the range

280   0-300 mA. All these instruments were connected to a PC with an IEEE488 bus and the test procedure was

281   controlled by a MATLAB script. Fig. 19 shows the output voltage normalized to the no-load value. In order

282   to improve the measurement accuracy, the voltage of each characterization point in Fig. 19 was obtained as a

283   mean of 100 measures.

284
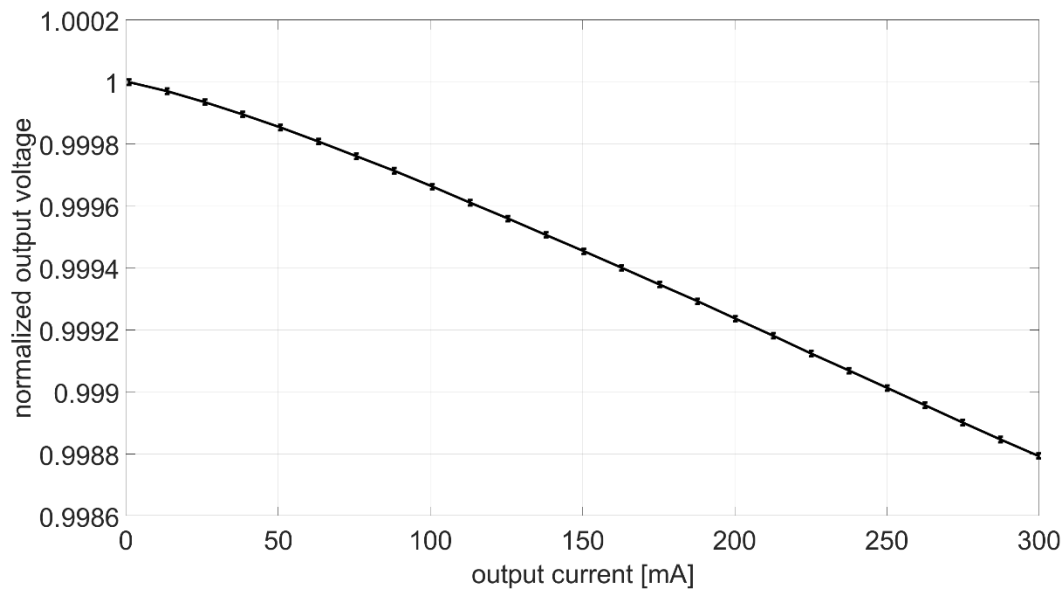
285

Fig.   19 –   Normalized output voltage of one reference generator module as a function of the load current

286   The relative variation in output voltage is less than 0.1% of the no-load value over the entire span of output

287   current. This variation is surely acceptable for the considered application, also given that almost all measures

288   are done in a ratiometric way, that is the excitation voltage of sensors is measured and used as a reference for

289   all measures. This measurement method also protects from the small reference voltage drift due to components

290   aging; thermal drifts are almost absent because temperature and humidity of the experiment are both controlled

291   by a dedicated HVAC (Heating,Ventilation and Air Conditioning) system which guarantees the temperature

292   stability in a range o +/- 0.5 °C around the nominal value of the test rooms.

293   Each cabinet contains also a PC-based DAQ system. Cabinets used for OT and DST contain a National

294   Instruments USB-6289 high accuracy multifunction DAQ, which has 18-bits nominal resolution on 16

295   multiplexed differential analog inputs, +/- 100 mV minimum voltage range and 500 kHz aggregated sample

296   rate. TT apparatus, instead, are served by Measurement Systems' Datascan 7220 DAQ units which have the

297   following characteristics: 14- or 16-bits software-selectable nominal resolution, 16 multiplexed differential

298   analog inputs, +/- 20 mV minimum voltage range and 40 Hz maximum aggregated sample rate. Each DAQ is

299   controlled by a personal computer through a USB 2.0 connection.

| 300 | IV. RESULTS AND UNCERTAINTY EVALUATION |

301 As proposed in [46], to validate the developed system several mechanical tests have been carried out on

302 different samples of soil. In this testing program automatic measurement from DST or OT have been compared,

303 with measurement taken with dial gauges firmly installed on the test apparatus. The relative deviation between

304 the output data of the displacement transducer and dial gauges were carefully monitored and checked. Fig. 20

305 shows the comparison between the two measurements for an OT. The data are presented in form of a typical

306 consolidation curve, or better, by plotting the thickness of the specimen against time. From the comparison, it

307 can be observed that there is an excellent compatibility between the two devices with the advantage, when

308 using the new system, of obtaining much more resolution, leading to a more accurate analysis.
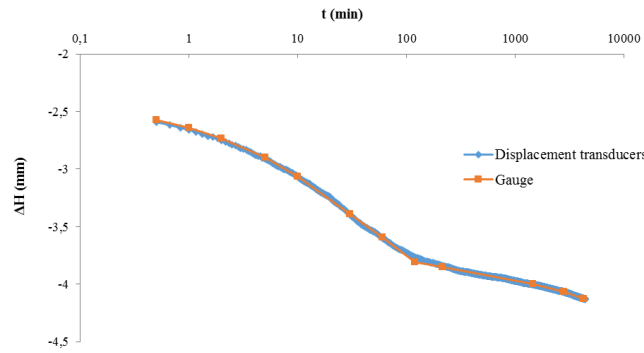
309

Fig. 20 – Consolidation curve obtained with dial gauge and LDT acquired with the proposed method

310 As an example, the uncertainty evaluation [47], [48] was performed considering different hardware

311 configurations reported in Table 1.

Table 1 – Hardware configuration for different geotechnical equipment

		OT	DST	TT
DAQ Board		NI 6289	NI 6289	DATASCAN 7220
Transducers	LDT (fully active 350 Ohm strain-gauge bridge)	APEK HS25B - 6433	APEK HS25B - 6433	
	LVDT			RDP LDC1000A
	Load Cell		DS-Europe 546Q-110 T-Hydronics TC-S AEP TCA AEP TCE	WF STALC3-3kN-21565 WF 4958-701501
	Pressure transducer			WF 17021 WF 17022 WF 17060 PDCR 810

312

313 The measurand value M is obtained from the acquired output sensed voltage (V_s) by means of the sensitivity

314 value (S):

$$M = \frac{V_s}{S} \tag{10}$$

315 Each transducer is affected by the its own errors like offset, gain, non-linearity or hysteresis that generally are
316 grouped in an overall error E_{tr} added (or subtracted) to the measurand. Moreover, the errors due to the DAQ
317 board E_{DAQ} that affect the acquired voltage should be taken in to account

$$M \pm E_{tot} = \frac{(V_s \pm E_{DAQ})}{S} \pm E_{tr} \tag{11}$$

318 To evaluate the total error E_{tot} for each test these two quantities must be estimated. Since the true value of
319 the measurand and of the errors is not known the corresponding uncertainties must be estimated. In this case a
320 pessimistic (Type B) evaluation has been made using only information from manuals and product specification
321 to have an idea of the metrological performance of the measurement system. Generally, no information is given
322 by the datasheets about the probability distribution of each error thus, a uniform distribution of each
323 contribution has been assumed to obtain the standard deviation and estimate the overall expanded uncertainty
324 with the 95% level of confidence

$$U_{tot_{95\%}} = k \cdot \sigma = 2 \cdot \sqrt{\left(\frac{U_{tr}}{\sqrt{3}}\right)^2 + \left(\frac{U_{DAQ}}{\sqrt{3} \cdot S}\right)^2} \tag{12}$$

325

326 For the sake of clarity in Tables 2 and 3 we report some uncertainty budget obtained using the mentioned
327 framework, although pessimistic, resulting in a very low value for overall uncertainty in all tests demonstrating
328 the goodness of choices and the high performance from the metrological point of view.

Table 2 - Uncertainty budget for OT using a NI USB 6289 in the full-scale range ±0.1 V

Transducer model, S/N	APEK HS25B, 6433 (Bridge 350 ohm)	
Supply voltage	10	V
FS range	25.8	mm
Linearity	0.1	+/- % FS
	25.8	μm
Output @ FS	7.2	mV/V
Sensitivity @ 5 V supply	5.58E-03	mV/μm
Max Output	72	mV
U_{tr}	14.90	μm
U_{DAQ}	0.008382014	mV
U_{DAQ}/S	1.50	μm

$U_{tot_{95\%}}$	29.94	µm

329

330

Table 3 - Uncertainty budget for DST load cells using a NI USB 6289 in the full-scale range ±0.1 V

Transducer model	AEP TCA (Bridge 350 ohm)	AEP TCE (Bridge 350 ohm)	
Supply Voltage	10	10	V
Full Scale (FS) range	50	500	kg
Non-linearity	0.03	0.03	% FS
Hysteresis	0.03	0.03	% FS
Repeatibility error	0.01	0.01	% FS
Output @ FS	2	2	mV/V
Sensitivity @ 10 V supply	4.00E-01	4.00E-02	mV/kg
Max Output	20	20	mV
U_{tr}	20.21	202.07	g
U_{DAQ}	0.008382014	0.008382014	mV
U_{DAQ}/S	0.06	0.58	kg
$U_{tot_{95\%}}$	0.06	0.58	kg

331

332 For example, the overall expanded uncertainty of the load cell AEP TCA (Full Scale range 50 kg) is equal to

333 60 g; this value is significantly lower than a reference value of 830 g evaluated experimentally using the same

334 transducer acquired by a previously existing system.

335

336   V.   CONCLUSIONS AND FUTURE WORKS

337 In the context of geotechnical trials, measurement is the major support for the analysis and decision-making,

338 since it concerns safety and risk assessment and allow to determine the establishment of special requirements

339 for decision support.

340 The GeoLab system shown in the present paper has been developed for the geotechnical laboratory activities,

341 in the context of a multidisciplinary investigation of a heavily polluted marine system, aimed at the

342 identification of the most sustainable strategies for the remediation and management of the environmental

343 contamination of the site. One of the goals of the interdisciplinary research program is the development of an

original system for acquisition, representation and analysis of the data coming from the geotechnical tests on the Mar Piccolo sediments (Taranto, South of Italy). The system is aimed to increase test speed, accuracy, and productivity and to reduce the probability of human mistakes. The realized framework, is reconfigurable and allows researchers to develop and test new procedures and to share data and results with other laboratories or research entities. Moreover, the design of a low noise power supply for transducers' excitation avoid the risk of measurement artefacts on acquired data while the use of data buffering strategy allows to have different rate in data consumption for different tests.

Other tasks have to be addressed, in the next future, to build a decision support tool such as the automatic identification of specific pattern features or profiles, using appropriate data processing and algorithms.

REFERENCES

[1] N. A. Cloete, R. Malekian, and L. Nair, "Design of Smart Sensors for Real-Time Water Quality Monitoring," IEEE Access, vol. 4, pp. 3975–3990, 2016.

[2] G. Andria, G. Cavone, V. D. Lecce, and A. M. L. Lanzolla, "Model characterization in measurements of environmental pollutants via data correlation of sensor outputs," IEEE Transactions on Instrumentation and Measurement, vol. 54, no. 3, pp. 1061–1066, Jun. 2005.

[3] H. B. Glasgow, J. M. Burkholder, R. E. Reed, A. J. Lewitus, and J. E. Kleinman, "Real-time remote monitoring of water quality: a review of current applications, and advancements in sensor, telemetry, and computing technologies," Journal of Experimental Marine Biology and Ecology, vol. 300, no. 1, pp. 409–448, Mar. 2004.

[4] C. Vitone, A. Federico, A. M. Puzrin, M. Ploetze, E. Carrassi, and F. Todaro, "On the geotechnical characterisation of the polluted submarine sediments from Taranto," Environ Sci Pollut Res, vol. 23, no. 13, pp. 12535–12553, Jul. 2016.

374 [5] F. Lamonaca, D. L. Carnì, M. Riccio, D. Grimaldi, and G. Andria, "Preserving Synchronization Accuracy
375   From the Plug-in of NonSynchronized Nodes in a Wireless Sensor Network," IEEE Transactions on
376   Instrumentation and Measurement, vol. 66, no. 5, pp. 1058–1066, May 2017.

377 [6] M. C. Falconi et al., "Design of an Efficient Pumping Scheme for Mid-IR Dy3+:Ga5Ge20Sb10S65 PCF
378   Fiber Laser," IEEE Photonics Technology Letters, vol. 28, no. 18, pp. 1984–1987, Sep. 2016.

379 [7] M. C. Falconi et al., "Dysprosium-Doped Chalcogenide Master Oscillator Power Amplifier (MOPA) for
380   Mid-IR Emission," Journal of Lightwave Technology, vol. 35, no. 2, pp. 265–273, Jan. 2017.

381 [8] Z. Lechowicz, A. Szymanski, and Baranski T., "Chapter 3 Laboratory investigations," in Developments
382   in Geotechnical Engineering, vol. 80, J. Hartlén and W. Wolski, Eds. Elsevier, 1996, pp. 85–136.

383 [9] N. Cardellicchio, C. Annicchiarico, A. D. Leo, S. Giandomenico, and L. Spada, "The Mar Piccolo of
384   Taranto: an interesting marine ecosystem for the environmental problems studies," Environ Sci Pollut Res,
385   vol. 23, no. 13, pp. 12495–12501, Jul. 2016.

386 [10]   M. Mali, M. M. Dell'Anna, M. Notarnicola, L. Damiani, and P. Mastrorilli, "Combining chemometric
387   tools for assessing hazard sources and factors acting simultaneously in contaminated areas. Case study:
388   'Mar Piccolo' Taranto (South Italy)," Chemosphere, vol. 184, pp. 784–794, Oct. 2017.

389 [11]   A. Federico, C. Vitone, and A. Murianni, "On the mechanical behaviour of dredged submarine clayey
390   sediments stabilized with lime or cement," Can. Geotech. J., vol. 52, no. 12, pp. 2030–2040, May 2015.

391 [12]   A. Federico, A. Murianni, G. Internò, E. Miccoli, C. Vitone, and M. Nobile, "Preliminary results on
392   the stabilization of dredged sediments from the Port of Taranto," presented at the Symposium on Coupled
393   Phenomena in Environmental Geotechnics from theoretical to experimental research to practical
394   applications. Coupled Phenomena in Environmental Geotechnics (CPEG),Manassero et al (Eds), 2013.

395 [13]   F. Sollecito, F. Cotecchia, M. Mali, D. Miccoli, and C. Vitone, "Geotechnical investigation of
396   submarine sediments for the environmental characterisation of a contaminated site," presented at the Proc.
397   2nd Symposium on Coupled Phenomena in Environmental Geotechnics (CPEG2), Leeds, UK, 2017.

398 [14]   F. Sollecito, "Geotechnical characterization of a polluted marine basin," PhD thesis, Polytechnic
399   University of Bari, Bari - Italy, 2018.

400 [15]   B. O. Vishwanath et al., "Development of Automated Laboratory based soil tester for qualification of
401   deepsea in-situ soil tester," in 2015 IEEE Underwater Technology (UT), 2015, pp. 1–10.

402 [16]   F. Adamo, G. Cavone, A. D. Nisio, A. M. L. Lanzolla, and M. Spadavecchia, "A proposal for an open
403   source energy meter," in 2013 IEEE International Instrumentation and Measurement Technology
404   Conference (I2MTC), 2013, pp. 488–492.

405 [17]   D. Lu, R. Challoo, P. V. Compton, and P. Leelani, "Design and development of an automated
406   geotechnical dynamic triaxial testing system," in AUTOTESTCON '91. IEEE Systems Readiness

407　　　Technology Conference. Improving Systems Effectiveness in the Changing Environment of the '90s,
408　　　Conference Record., 1991, pp. 405–409.

409　[18]　R. M. Zimmerman, "Geotechnical Instrumentation Requirements for at-Depth Testing and Repository
410　　　Monitoring in TUFF," IEEE Transactions on Nuclear Science, vol. 30, no. 1, pp. 556–560, Feb. 1983.

411　[19]　E. Selig and M. Silver, "Automated Data Acquisition, Transducers, and Dynamic Recording for the
412　　　Geotechnical Testing Laboratory," Geotechnical Testing Journal, vol. 2, no. 4, p. 185, 1979.

413　[20]　M. M. Monkul and O. Önal, "A Visual Basic program for analyzing oedometer test results and
414　　　evaluating intergranular void ratio," Computers & Geosciences, vol. 32, no. 5, pp. 696–703, Giugno 2006.

415　[21]　H. G. Ramos, M. Trindade, and A. C. Serra, "A measurement system to automate laboratory testing in
416　　　soils," in , IEEE Instrumentation and Measurement Technology Conference, 1997. IMTC/97. Proceedings.
417　　　Sensing, Processing, Networking, 1997, vol. 2, pp. 1048–1051 vol.2.

418　[22]　"Automatic triaxial tests system - AUTOTRIAX 2, Soil mechanics testing equipment, Controls." .

419　[23]　"System for the Characterization of Soil Samples through Cyclical and Dynamic Tests based on
420　　　CompactRIO and LabVIEW - Solutions - National Instruments." .

421　[24]　F. Adamo, F. Attivissimo, A. Di Nisio, M. Savino, and M. Spadavecchia, "A spectral estimation
422　　　method for nonstationary signals analysis with application to power systems," Measurement, vol. 73, pp.
423　　　247–261, Sep. 2015.

424　[25]　J. H. Atkinson and P. L. Bransby, The mechanics of soils : an introduction to critical state soil
425　　　mechanics. London : McGraw-Hill, 1978.

426　[26]　R.F. Craig, Craig's Soil Mechanics, Seventh Edition. CRC Press, 2004.

427　[27]　H. K. H. Head and R. J. Epps, Manual of Soil Laboratory Testing, 3rd edition, Vol. II: Permeability,
428　　　Shear Strength and Compressibility Tests. Whittles Publishing, 2011.

429　[28]　"BSI (1990) BS 1377: 1990—Methods of Test for Soils for Civil Engineering Purposes.　Milton
430　　　Keynes." 1990.

431　[29]　"ASTM D2435 / D2435M-11, Standard Test Methods for One-Dimensional Consolidation Properties
432　　　of Soils Using Incremental Loading, ASTM International, West Conshohocken, PA, 2011,
433　　　www.astm.org." .

434　[30]　A. Bishop and D. J. Henkel, Measurement of Soil Properties in the Triaxial Test. London: Edward
435　　　Arnold (Publishers) LTD, 1962.

436　[31]　"ASTM D3080 / D3080M-11, Standard Test Method for Direct Shear Test of Soils Under
437　　　Consolidated Drained Conditions, ASTM International, West Conshohocken, PA, 2011, www.astm.org.".

438   [32]   "ASTM D4767-11, Standard Test Method for Consolidated Undrained Triaxial Compression Test for
439   Cohesive Soils, ASTM International, West Conshohocken, PA, 2011, www.astm.org." .

440   [33]   D. M. Wood, Soil Behaviour and Critical State Soil Mechanics. Cambridge University Press, 1991.

441   [34]   E. J. Rueda, S. Caro, B. Caicedo, and J. Monroy, "A new approach for the advanced mechanical
442   characterisation of asphalt mixtures using the hollow cylinder methodology," Measurement, vol. 103, pp.
443   333–342, Jun. 2017.

444   [35]   G. Andria, A. Baccigalupi, M. Borsic, P. Carbone, P. Daponte, C. De Capua, A. Ferrero, D. Grimaldi,
445   N. Locci, A. M. L. Lanzolla, D. Macii, C. Muscas, L. Peretto, D. Petri, S. Rapuano, M. Riccio, S. Salicone,
446   F. Stefan, "Remote Didactic Laboratory 'G. Savastano'; The Italian Experience for E-Learning at the
447   Technical Universities in the Field of Electrical and Electronic Measurement: Architecture and
448   Optimization of the Communication Performance Based on Thin Client Technology," IEEE Transactions
449   on Instrumentation and Measurement, vol. 56, no. 4, pp. 1124–1134, Aug. 2007.

450   [36]   G. Andria, A. Baccigalupi, M. Borsic, P. Carbone, P. Daponte, C. De Capua, A. Ferrero, D. Grimaldi,
451   N. Locci, A. M. L. Lanzolla, D. Macii, C. Muscas, L. Peretto, D. Petri, S. Rapuano, M. Riccio, S. Salicone,
452   F. Stefan, "Remote Didactic Laboratory 'G. Savastano'; The Italian Experience for E-Learning at the
453   Technical Universities in the Field of Electrical and Electronic Measurements: Overview on Didactic
454   Experiments," IEEE Transactions on Instrumentation and Measurement, vol. 56, no. 4, pp. 1135–1147,
455   Aug. 2007.

456   [37]   F. Adamo, F. Attivissimo, and M. Spadavecchia, "A tool for Photovoltaic panels modeling and
457   testing," in 2010 IEEE Instrumentation Measurement Technology Conference Proceedings, 2010, pp.
458   1463–1466.

459   [38]   G. Andria, F. Attivissimo, A. Di Nisio, A. M. L. Lanzolla, and A. Pellegrino, "Development of an
460   automotive data acquisition platform for analysis of driving behavior," Measurement, vol. 93, pp. 278–
461   287, Nov. 2016.

462   [39]   F. Attivissimo, A. D. Nisio, C. G. C. Carducci, and M. Spadavecchia, "Fast Thermal Characterization
463   of Thermoelectric Modules Using Infrared Camera," IEEE Transactions on Instrumentation and
464   Measurement, vol. 66, no. 2, pp. 305–314, Feb. 2017.

465   [40]   F. Attivissimo, C. Guarnieri Calò Carducci, A. M. L. Lanzolla, and M. Spadavecchia, "An Extensive
466   Unified Thermo-Electric Module Characterization Method," Sensors (Basel), vol. 16, no. 12, Dec. 2016.

467   [41]   M. G. Angelini, D. Costantino, and A. D. Nisio, "ASTER image for environmental monitoring Change
468   detection and thermal map," in 2017 IEEE International Instrumentation and Measurement Technology
469   Conference (I2MTC), 2017, pp. 1–6.

[42] D. Constantino and M. G. Angelini, "Thermal monitoring using an ASTER image," JARS, JARSC4, vol. 10, no. 4, p. 46031, Dec. 2016.

[43] "TL1431 Precision Adjustable (Programmable) Shunt Reference, TI.com." [Online]. Available: http://www.ti.com/product/tl1431/description?keyMatch=TL1431&tisearch=Search-EN-Everything. [Accessed: 21-May-2018].

[44] "TLV1117 Single Output LDO, 800mA, Fixed and Adj., Internal Current limit, Thermal Overload Protection, TI.com." [Online]. Available: http://www.ti.com/product/tlv1117?keyMatch=TLV1117&tisearch=Search-EN-Everything. [Accessed: 21-May-2018].

[45] "VPG - Foil Resistors - 300144Z & 300145Z (Z-Foil)." [Online]. Available: http://www.vishaypg.com/foil-resistors/list/product-63115/. [Accessed: 11-May-2018].

[46] H. Shen, W. Haegeman, and H. Peiffer, "3D Printing of an Instrumented DMT: Design, Development, and Initial Testing," GTJ, vol. 39, no. 3, pp. 492–499, Mar. 2016.

[47] R. Kumar and K. Bhargava, "Review of Evaluation of Uncertainty in Soil Property Estimates from Geotechnical Investigation," in Advances in Structural Engineering, Springer, New Delhi, 2015, pp. 2545–2550.

[48] S. Pytharouli, S. Chaikalis, and S. C. Stiros, "Uncertainty and bias in electronic tide-gauge records: Evidence from collocated sensors," Measurement, vol. 125, pp. 496–508, Sep. 2018.